AD-A092 140 NAVAL POSTGRADUATE SCHOOL MONTEREY CA F/G 17/5
MEASUREMENT OF PERFORMANCE PARAMETERS FOR A FLIR THERMAL IMAGIN--ETC(U)
JUN 80 W L SELLERS

UNCLASSIFIED NL

1 OF 1
AD
A092140

END
DATE
FILMED
1 81
DTIC

AD A092140

# NAVAL POSTGRADUATE SCHOOL

## Monterey, California

LEVEL II

DTIC
1980

# THESIS

MEASUREMENT OF PERFORMANCE PARAMETERS
FOR A FLIR THERMAL IMAGING SYSTEM

by

William Lester Sellers

June 1980

145

Thesis Advisor: E. C. Crittenden, Jr.

Approved for public release; distribution unlimited

DDC FILE COPY

251450
81 11 24 086

SECURITY CLASSIFICATION OF THIS PAGE (When Data Entered)

# REPORT DOCUMENTATION PAGE

READ INSTRUCTIONS BEFORE COMPLETING FORM

1. REPORT NUMBER

2. GOVT ACCESSION NO. AD-A092 140

3. RECIPIENT'S CATALOG NUMBER

4. TITLE (and Subtitle)

Measurement of Performance Parameters for a FLIR Thermal Imaging System

5. TYPE OF REPORT & PERIOD COVERED

Master's Thesis; June 1980

6. PERFORMING ORG. REPORT NUMBER

7. AUTHOR(s)

William Lester Sellers

8. CONTRACT OR GRANT NUMBER(s)

9. PERFORMING ORGANIZATION NAME AND ADDRESS

Naval Postgraduate School
Monterey, California 93940

10. PROGRAM ELEMENT, PROJECT, TASK AREA & WORK UNIT NUMBERS

11. CONTROLLING OFFICE NAME AND ADDRESS

Naval Postgraduate School
Monterey, California 93940

12. REPORT DATE

June 1980

13. NUMBER OF PAGES

44

14. MONITORING AGENCY NAME & ADDRESS(if different from Controlling Office)

15. SECURITY CLASS. (of this report)

Unclassified

15a. DECLASSIFICATION/DOWNGRADING SCHEDULE

16. DISTRIBUTION STATEMENT (of this Report)

Approved for public release; distribution unlimited.

17. DISTRIBUTION STATEMENT (of the abstract entered in Block 20, if different from Report)

18. SUPPLEMENTARY NOTES

19. KEY WORDS (Continue on reverse side if necessary and identify by block number)

NPS FLIR
thermal imaging
IR imaging performance parameters

20. ABSTRACT (Continue on reverse side if necessary and identify by block number)

The performance parameters of Noise Equivalent Temperature Difference (NETD), Minimum Resolvable Temperature Difference (MRTD), and Minimum Detectable Temperature Difference (MDTD) for the Naval Postgraduate School FLIR thermal imaging system were measured. The effects on these parameters of varying the detector aperture size (pinhole) were studied. It was determined that the thermal sensitivity of the system was directly proportional to the pinhole radius

DD FORM 1 JAN 73 1473 (Page 1)

EDITION OF 1 NOV 65 IS OBSOLETE
S/N 0102-014-6601



SECURITY CLASSIFICATION OF THIS PAGE (When Data Entered)

Block #20 cont'd

and resolution of the system was inversely proportional to the pinhole radius. Minimum values obtained were: NETD = 3.08°C, MRTD = 18°C, MDTD = 16°C.

Accession For
NTIS GRA&I X
DTIC TAB
Unannounced
Justification
By
Distribution/
Availability Codes
Dist
A

Approved for public release; distribution unlimited

# Measurement of Performance Parameters for a FLIR Thermal Imaging System

by

William Lester Sellers
Lieutenant Commander, United States Navy
B.S., United States Naval Academy, 1968

Submitted in partial fulfillment of the requirements for the degree of

MASTER OF SCIENCE IN PHYSICS

from the

NAVAL POSTGRADUATE SCHOOL
June 1980

Author: William L. Sellers

Approved by: Eugene C. Crittenden Jr., Thesis Advisor

Edmund A. Milne, Second Reader

J. N. Dyer, Chairman, Department of Physics and Chemistry

William M. Tolles, Dean of Science and Engineering

ABSTRACT

The performance parameters of Noise Equivalent Temperature Difference (NETD), Minimum Resolvable Temperature Difference (MRTD), and Minimum Detectable Temperature Difference (MDTD) for the Naval Postgraduate School FLIR thermal imaging system were measured. The effects on these parameters of varying the detector aperture size (pinhole) were studied. It was determined that the thermal sensitivity of the system was directly proportional to the pinhole radius and resolution of the system was inversely proportional to the pinhole radius. Minimum values obtained were: NETD = 3.08° C, MRTD = 18° C, MDTD = 16° C.

TABLE OF CONTENTS


I. INTRODUCTION ---------- 10

A. BACKGROUND ---------- 10

B. OBJECTIVES ---------- 11

II. THEORY ---------- 13

A. DETECTOR PARAMETERS ---------- 13

B. SYSTEM PARAMETERS ---------- 14

1. Noise Equivalent Temperature Difference 15

2. Minimum Resolvable Temperature Difference ---------- 17

3. Minimum Detectable Temperature Difference ---------- 20

III. EXPERIMENTAL PROCEDURE ---------- 22

A. APPARATUS USED FOR EVALUATION ---------- 22

1. The FLIR ---------- 22

2. Test Equipment ---------- 26

B. MEASUREMENT PROCEDURE ---------- 28

1. Noise Measurement ---------- 28

2. NETD Measurement ---------- 28

3. MRTD Measurement ---------- 30

4. MDTD Measurement ---------- 32

IV. PRESENTATION OF DATA ---------- 33

A. NETD DATA ---------- 33

B. MDTD DATA ---------- 33

C. MRTD DATA ---------- 34

D. THEORETICAL VALUES ---------- 39

V. CONCLUSIONS ---------- 41

A. SUMMARY ---------- 41

B. COMMENT ---------- 42

BIBLIOGRAPHY ---------- 43

INITIAL DISTRIBUTION LIST ---------- 44

LIST OF TABLES

I. FLIR Electronic Components ---------- 24

II. NETD Data ---------- 33

III. MDTD Data ---------- 33

IV. MTS Data ---------- 34

V. MRTD Data ---------- 34

VI. Theoretical NETD Values ---------- 39

VII. Theoretical MRTD Values ---------- 40

LIST OF FIGURES


1. MRTD Targets ---------- 19
2. Typical Shape of MRTD Curve ---------- 19
3. Dahl-Kirkham telescope ---------- 23
4. Mirror scanning system ---------- 23
5. HgCdTe Detector and Dewar Diagram ---------- 25
6. Circuit for HgCdTe Photoconductive Cell --------- 25
7. Heating Element ---------- 27
8. Test Targets ---------- 27
9. Detector Mounting Tube ---------- 29
10. NETD Test Pattern and Waveform ---------- 31
11. NETD Results ---------- 35
12. MDTD Results ---------- 36
13. Signal Strength Versus Temperature ---------- 37
14. MRTD Results ---------- 38

ACKNOWLEDGEMENT

I am indebted to a number of people for their help and guidance on this project. I wish to acknowledge Mr. Bob Moeller and Mr. Ken Smith for their assistance with the mechanical structures and electronic components respectively.

I would like to specially thank Professor Eugene Crittenden whose wisdom and guidance were invaluable in the preparation of this thesis.

I would like to thank my wife, Ginny, for her love, devotion, and typing of the rough draft.

Finally, I would like to express my grateful thanks to the Creator of the universe who "sees everything under the heavens", and without whom this thesis would not be possible.

# I. INTRODUCTION

## A. BACKGROUND

A thermal imaging system is a device which converts radiation in the far infrared to visible radiation in such a way that information can be extracted from the resulting image. Thermal imaging systems extend our vision beyond the visible red into the far infrared by making use of the radiation naturally emitted by warm objects. In addition, the advantage of the infrared wavelengths of the electromagnetic spectrum lies in their ability to penetrate atmospheric aerosols, such as fog or rain, better than visible radiation. Thermal imagers can be used for medical diagnosis, nondestructive testing of materials, real time aircraft reconnaissance, imaging extraterrestrial objects, weather mapping, and night vision.

Real time thermal infrared imagers which utilize optical-mechanical scanning devices to convert infrared to visible information are known by the term FLIR, which is an acronym for Forward Looking Infra-Red. It is used to denote any fast framing thermal imager that provides an update rate comparable to that of television.

A FLIR works in the following manner. An optical system collects, filters and focuses infrared radiation through a mechanical scanning system which moves the image across an

infrared detector. The detector output is an electrical signal that is proportional to the scene radiance. The electrical signal is then processed for display on a video monitor, much like a television.

At the Naval Postgraduate School an experimental FLIR has been designed and constructed from available components at the school. It is a working model that can provide a basic knowledge of the problems and principles of a FLIR system. A study of the basic elements of this FLIR system has been conducted [Gruber, 1979].

It is important to be able to evaluate the performance of a complete thermal imaging system. The major parameters which are chosen to characterize the performance of a system are: Noise Equivalent Temperature Difference (NETD), Modulation Transfer Function (MTF), Minimum Resolvable Temperature Difference (MRTD), Minimum Detectable Temperature Difference (MDTD) and Signal Transfer Function (SiTF). It has been pointed out that only three of the above parameters are generally believed to provide a good first order estimate of thermal imaging system quality. These are MTF, NETD and MRTD [Lloyd, 1975].

## B. OBJECTIVES

There is much to be gained from a study of the fundamental image quality parameters which are applicable to FLIR. It is the objective of this thesis project to measure and

evaluate the key performance parameters of noise equivalent temperature difference (NETD) and minimum resolvable temperature difference (MRTD) for the Naval Postgraduate School FLIR and to compare these results to their theoretical ideal values. A second objective is to investigate the effect of changing the detector aperture size on overall system performance.

## II. THEORY

### A. DETECTOR PARAMETERS

The heart of a thermal imaging FLIR is its infrared detector. An infrared detector under a particular set of operating conditions is characterized by two parameters: responsivity R and the specific detectivity D*. Responsivity is the response of the detector expressed in volts of output per watt of input signal. It is defined as

$$R = \frac{V_s}{HA_d}$$

where

$V_s$ = signal voltage ($V_{rms}$)

$H$ = value of the irradiance ($\frac{W}{cm^2}$)

$A_d$ = detector area ($cm^2$)

The specific detectivity is the detector output signal-to-noise ratio for one watt of input signal, normalized to a unit detector sensitive area, and a unit electrical bandwidth. It is defined as

$$D^* = \frac{(A_d\ \Delta f)^{\frac{1}{2}}\ V_s}{HA_d\ V_n} = \frac{R(A_d\ \Delta f)^{\frac{1}{2}}}{V_n}$$

where

$V_n$ = noise voltage ($V_{rms}$)

$\Delta f$ = electrical bandwidth (Hz)

The determination of the value of these parameters is not within the scope of this project but were measured for the HgCdTe detector used in the FLIR by [Kunz, 1974].

## B. SYSTEM PARAMETERS

System parameters fall into two categories, objective and subjective. The objective system parameters include signal transfer function (SiTF), modulation transfer function (MTF) and noise equivalent temperature difference (NETD). The subjective system parameters are minimum resolvable temperature difference (MRTD) and minimum detectable temperature difference (MDTD). These parameters can all be measured in the laboratory and must satisfy two basic requirements. First, they must be capable of well defined and repeatable measurement. Secondly, they must correlate well to the field performance of the system, which for a military system might be measured in terms of recognition or detection range for a given target [Newbery and Worsick, 1976]. It should be noted that there is an important difference between a thermal imaging system and most visual optical devices. The field performance of a FLIR is limited as much by thermal noise (temperature sensitivity) as by spatial resolution. Thus the need for these properties to be combined into a unified system-observer performance criterion. This is what is meant by subjective parameters, ones in which the spatial and temporal integration effects of the eye of the observer are taken into account.

1. Noise Equivalent Temperature Difference

The oldest and most widely used measure of the ability of a system to discriminate small signals in noise is the noise equivalent temperature difference (NETD). It is defined as the blackbody target to background temperature difference required to produce a unity signal-to-noise ratio at some measuring point in the sensor, for example on the video signal before the display [Lloyd 1975].

The derivation of NETD has been done by a number of authorities, among them are [Lloyd, 1975], [Klein, 1976] and [Dereniak and Brown, 1975]. The principle assumptions involved in the derivation are important to know in order to have a good understanding of the significance of NETD. Lloyd presents the following assumptions in his derivation:

a. The detector responsivity is uniform over the detector's rectangular sensitive area.

b. The detector D* is independent of other factors in the NETD equation.

c. Atmospheric transmission losses between the target and the sensor are negligible.

d. The target and background are blackbodies.

e. The detector angle subtense, the target angle subtense, and the inverse of the collecting optic focal ratio can be approximated as small angles.

f. The electronic processing introduces no noise.

g. $\frac{\partial W_\lambda}{\partial T} \approx \frac{C_2}{\lambda T_b^{\,2}}$

h. $D^*(\lambda) = \left(\frac{\lambda}{\lambda_p}\right) D^*(\lambda_p)$

The resulting formula for NETD can be stated as:

$$\mathrm{NETD} = \frac{\pi\sqrt{A_d \Delta f_r}\ \lambda_p\ T_b^{\,2}}{\alpha\beta A_o \tau_o D^*(\lambda_p) C_2 \int_{\lambda_1}^{\lambda_2} W_\lambda(T_b)\,d\lambda}$$

where

$A_d$ = detector area ($cm^2$)

$\Delta f_r$ = equivalent noise bandwidth (Hz)

$\lambda_p$ = wavelength at the peak of spectral response of the detector ($\mu m$)

$T_b$ = background temperature (°K)

$\alpha, \beta$ = detector angular subtenses (radians)

$A_o$ = effective collecting area of the infrared optics, including obscuration ($cm^2$)

$\tau_o$ = infrared optical transmission coefficient

$D^*(\lambda_p)$ = peak spectral detectivity $\left(\frac{cm\ Hz^{1/2}}{watt}\right)$

$C_2$ = $1.4388 \times 10^4\ \mu m\ °K$

$\int_{\lambda_1}^{\lambda_2} W_\lambda\,d\lambda$ = effective spectral radiant emittance $\left(\frac{watt}{cm^2}\right)$

The parameter NETD is not a good image quality summary measure. It does not always correlate well with the field performance of the system because the observer

can carry out spatial and temporal integration on the displayed image. Hence this effectively improves the signal-to-noise ratio and therefore the temperature resolution. However, the NETD is a good measure of sensor performance and is a good sensitivity diagnostic test.

2. Minimum Resolvable Temperature Difference

The minimum resolvable temperature difference (MRTD) is a more difficult quantity to formalize. As a subjective system parameter, the MRTD is a measure for the signal-to-noise-ratio limited thermal sensitivity of a system as a function of spatial frequency. It is defined as the image signal-to-noise ratio required for an observer to resolve a four bar target that is masked by noise. The derivation for MRTD by Lloyd uses the same assumptions as for NETD, supplemented by the following:

a. The effect of temporal integration by the observer is approximated by a fixed integration time of 0.2 seconds. It is assumed that the eye adds signals linearly and takes the root-mean-square value of noise within any 0.2 second interval.

b. The effect of narrowband spatial filtering in the eye in the presence of a periodic square bar target of frequency $f_T$ is approximated by a postulated matched filter for a single bar.

c. The electronic processing and monitor are assumed to be noiseless.

d. The system is relatively simple with zero overscan, a well-behaved MTF, and a well-behaved noise power spectrum.

e. The system is operated linearly so that the response to the target is describable by the MTF.

f. The image formation is assumed to be spatially invariant in the scan direction.

g. The displayed noise is white within the signal band pass.

h. There is a 90 percent probability of individual bar detection.

The derived expression for MRTD is:

$$\mathrm{MRTD} = \frac{3(\mathrm{NETD}/\Delta f_R)\, f_T \left(\frac{\alpha\beta}{\tau_d}\right)^{\frac{1}{2}}}{r_s\, (T_e \dot{F})^{\frac{1}{2}}}$$

where

$f_T$ = fundamental target frequency $\left(\frac{cy}{mrad}\right)$

$T_e$ = effective eye integration time (sec)

$\tau_d$ = detector dwelltime (sec)

$\dot{F}$ = frame rate (Hz)

$r_s$ = overall system MTF

An example of a series of four bar targets is shown in Figure 1, while the general shape of the MRTD curve is shown in Figure 2.

The MRTD concept is a useful analytical and design tool which is indicative of system performance in recognition

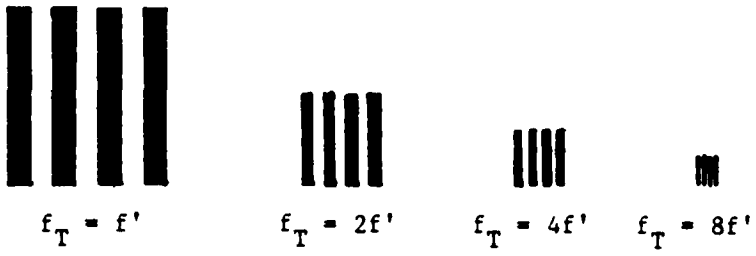


Figure 1. MRTD targets

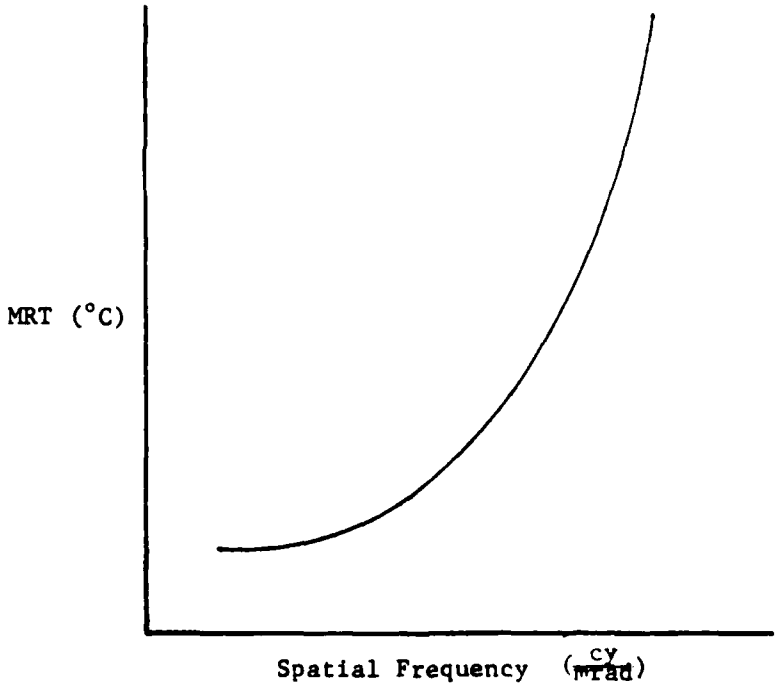


Figure 2. Typical shape of MRTD curve

tasks. It is widely accepted because it is an easily grasped, clearly observable concept.

3. Minimum Detectable Temperature Difference

The parameter of minimum detectable temperature difference (MDTD) is at present not widely accepted and no conventions for it exist. Nonetheless, it is a useful concept and is designed to correlate with noise-limited field detection performance. The MDTD is defined as the blackbody temperature difference required for an observer to detect the presence of a square target when he is allowed unlimited time to make a decision and knows where to look for the target.

In deriving the MDTD equation, the same assumptions which were previously stated for NETD and MRTD still apply. The target is a square blackbody with variable dimension W set against a large uniform background. From Lloyd the derived expression for MDTD is:

$$\mathrm{MDTD}\ \left(f_T=\frac{1}{2W}\right) = \frac{r_s\ 1.5\sqrt{2}\ \mathrm{MRTD}\ \left(f_T=\frac{1}{2W}\right)}{\overline{I(x,y)}}$$

where $\overline{I(x,y)}$ = the average value of the convolution integral of the image of the square target.

The difficulty of accurately predicting MDTD arises from the necessity to calculate the quantity $\overline{I(x,y)}$. It can be seen from the above relationship that MDTD is the aperiodic equivalent of MRTD, and is usually plotted as a function of the inverse of target size [Newbery and Worswick, 1976].

It can also be seen that unlike MRTD, MDTD does not have a limiting value of target size, as very small targets can be detected, if they are hot enough. It is this property that correlates well with the practice of occluding the sensitive area of the infrared detector by means of a focal plane baffle or "pinhole". The effect is the same in either case because the solid angle subtended by the detector is reduced and hence less power is received. On the other hand, by decreasing the size of a detector pinhole, the resolution of the system is increased. The tradeoff implications for the FLIR designer are clear: the thermal sensitivity of the system can be increased at the expense of decreasing the spatial resolution, all by means of adjusting the pinhole size. The MDTD parameter can be made to show this relationship by plotting it as a function of the spatial cutoff frequency of the pinhole.

## III. EXPERIMENTAL PROCEDURE

### A. APPARATUS USED FOR EVALUATION

#### 1. The FLIR

The FLIR to be evaluated is a single cell, serially scanned thermal imaging system. The optics consisted of a 15.24 cm diameter Cassegrainian type reflecting astronomical telescope with an equivalent focal length of 228.6 cm. The Cassegrainian type telescope has a central obscuration, an adjustable spherical primary mirror, a fixed ellipsoidal secondary mirror, and a total collecting area of 172.8 $cm^2$. This type of telescope is called a Dahl-Kirkham and is shown in Figure 3. Mounted to the back end of the telescope is the scanning mechanism. The scanning devices are two oscillating plane mirrors manufactured by General Scanning, Inc. These mirrors are mounted at a 45° angle to the beam exiting from the telescope and are mutually perpendicular to each other. Thus the beam is directed to the detector while the motion of the mirrors moves the image in a raster pattern. This process is depicted in Figure 4. The horizontal scan rate is 200 Hz and the vertical frame rate is .5 Hz. This produces an image with 300 lines per picture height. The detector for the FLIR is a 2mm square mercury cadmium telluride (HgCdTe) single cell detector manufactured by Santa Barbara Research, Inc. It is mounted in a side-looking

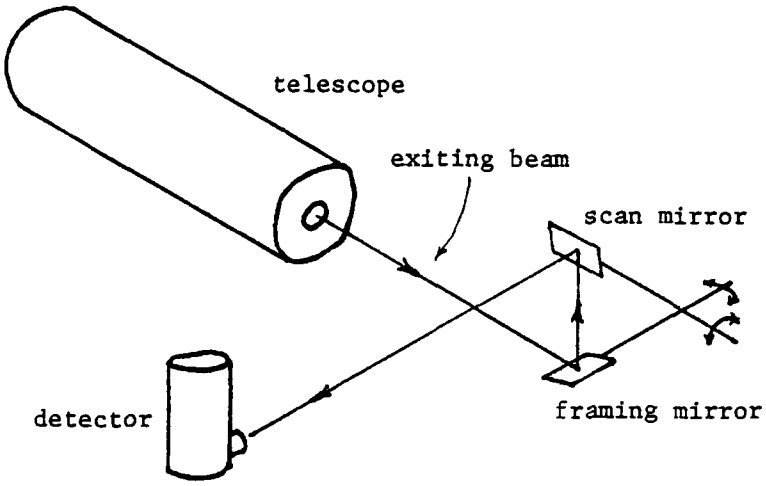


Figure 4. Mirror scanning system

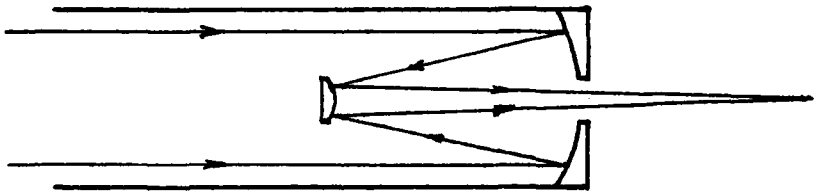

Figure 3. Dahl-Kirkham telescope

dewar and utilizes liquid nitrogen cooling to 77° K. The detector operates in the 8-14 μm region and is equipped with an IRTRAN 4 window. See Figure 5.

The electronic equipment for the FLIR serves two functions. The mirror scan drive equipment provides drive power signals to the mirrors and scan control signals to the video system. The video equipment detects, amplifies, filters and displays the signals from the detector. Since the HgCdTe detector is used as a photoconductor, a special circuit is needed to provide the conduction current. Figure 6 details this circuit.

Table I provides a listing of the electronic equipment and its use.

Table I. FLIR Electronic Components

| Scanning Equipment | Use |
|---|---|
| Hewlett Packard 3310 Function Generator | Raster control |
| General Scanning CCX101 Scanner Control | Horizontal Mirror Drive |
| Hewlett Packard 467A Power Amplifier | Vertical Mirror Drive |
| Wavetek 180 Function Generator | Raster Control |
| **Video Equipment** | **Use** |
| Princeton Applied Research Model 113 Preamplifier | Detector Signal Amplifier |
| Hewlett Packard 465 A Power Amplifier | Video Signal Amplifier |

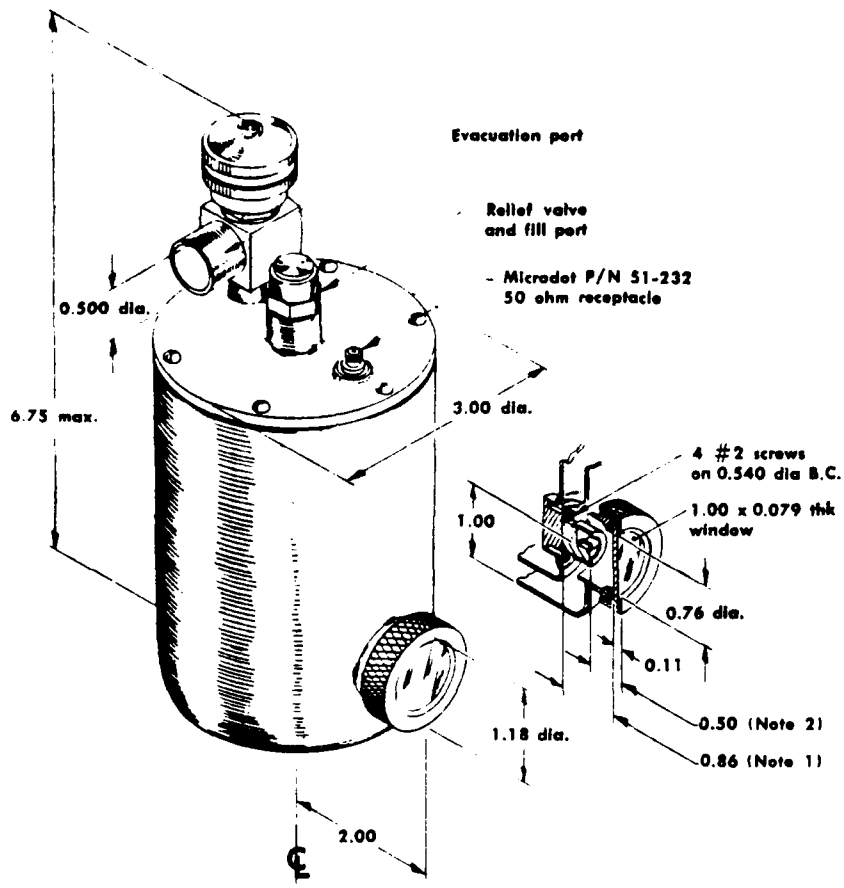


Figure 5. HgCdTe Detector and dewar diagram

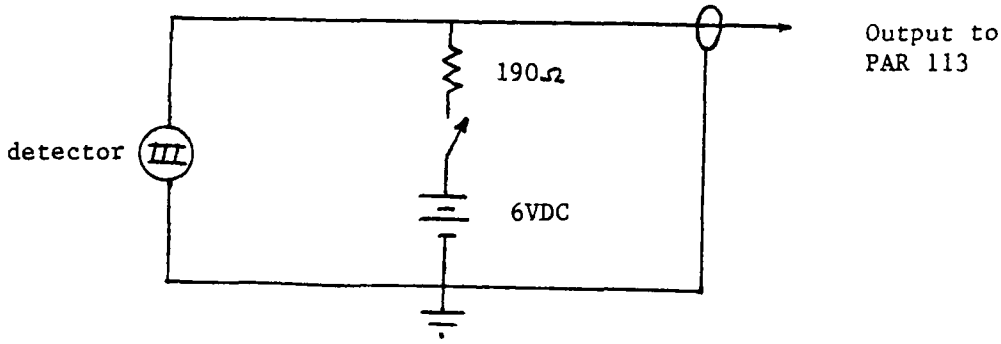


Figure 6. Circuit for HgCdTe photoconductive cell

| | |
|---|---|
| Monsanto OS-226 (P)/USM-368 Oscilloscope | Display |
| Interstate Elect. Corp. P12 Pulse Generator | Flyback blanking |
| Hewlett Packard 467A Power Amplifier | Blanking Signal Amplifier |

2. Test Equipment

The test equipment required to conduct the performance parameter measurements was relatively easy to assemble, set up and use. A blackbody heat source was required for all three tests. It consisted of a 300 watt U-shaped heating element with a long, flat aluminum bar attached to it. See Figure 7. The bar was painted flat black and had a chromel-alumel thermocouple attached to its front surface. A power-stat controlled the temperature of the heating element. The thermocouple was connected to a galvanometer capable of reading to hundredths of a millivolt. The resulting thermocouple temperature accuracy was $\pm .1°C$.

The targets utilized for the tests were simply pieces of cardboard with various size shapes cut out of them, according to the test being conducted. These were placed at the heat source, between it and the FLIR, to act as a baffle. Since the total field of view of the FLIR fully encompassed the target/baffle, the background was uniform and the thermal radiation could only pass through the slits. See Figure 8.

There was one piece of hardware especially designed and built in order to modify the FLIR for the parameter

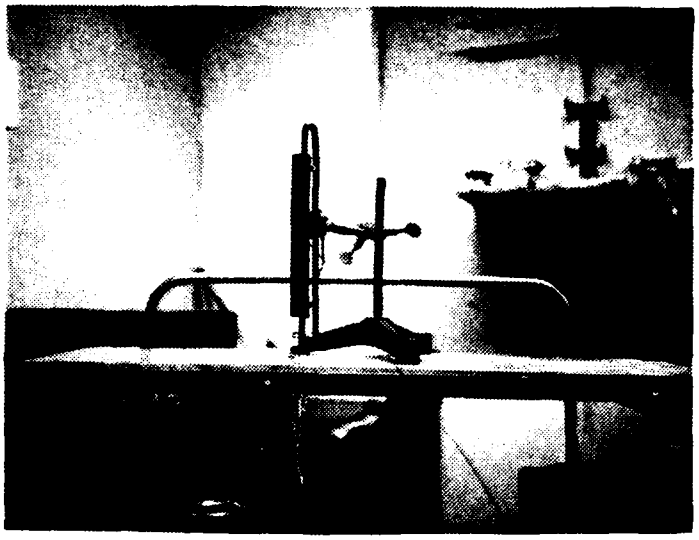

Figure 7. Heating element

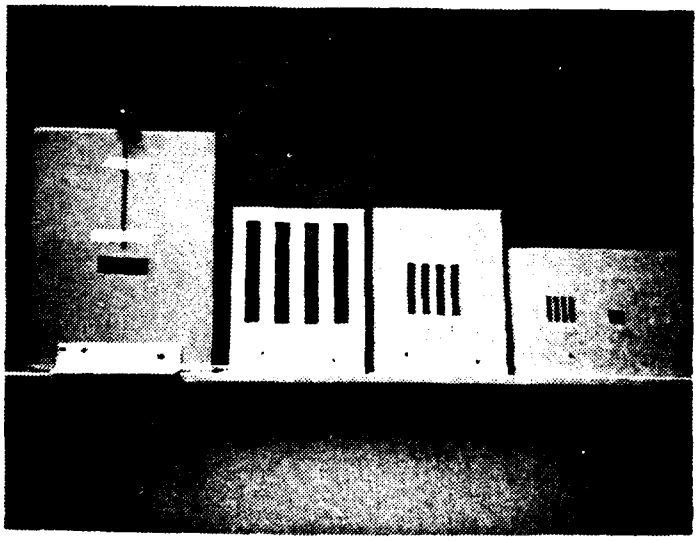

Figure 8. Test targets

testing. The original detector mounting device was inadequate in that there was no means to install a pinhole in the optical path. The replacement mounting tube utilized two germanium lenses as field lenses to image the pinhole onto the detector. Figure 9 is a diagram of the detector mounting tube. Another feature of the tube was the pinhole holder allowed for quick and easy change of pinhole sizes. Each pinhole size had its own holder. Pinhole sizes used were .368 mm, .50 mm, .75 mm, 1.00 mm and 1.5 mm.

## B. MEASUREMENT PROCEDURE

### 1. Noise Measurement

The first task in the evaluation process was to determine the noise level in the system. It was found that initially there was a great deal of undesirable noise at an unacceptably high level that had to be eliminated. This was accomplished by means of proper electrical grounding and shielding of the components. It was this effort to reduce the noise that led to the installation of the phenolic insert in the mounting tube. This electrically isolated the detector from all other components. The noise level was measured by a Hewlett-Packard 3400A RMS Voltmeter from the output of the PAR 113 amplifier. With the amplifier gain set at 1000, the background noise voltage level $V_s$ was measured.

### 2. NETD Measurement

To measure the value of NETD, a test pattern similar

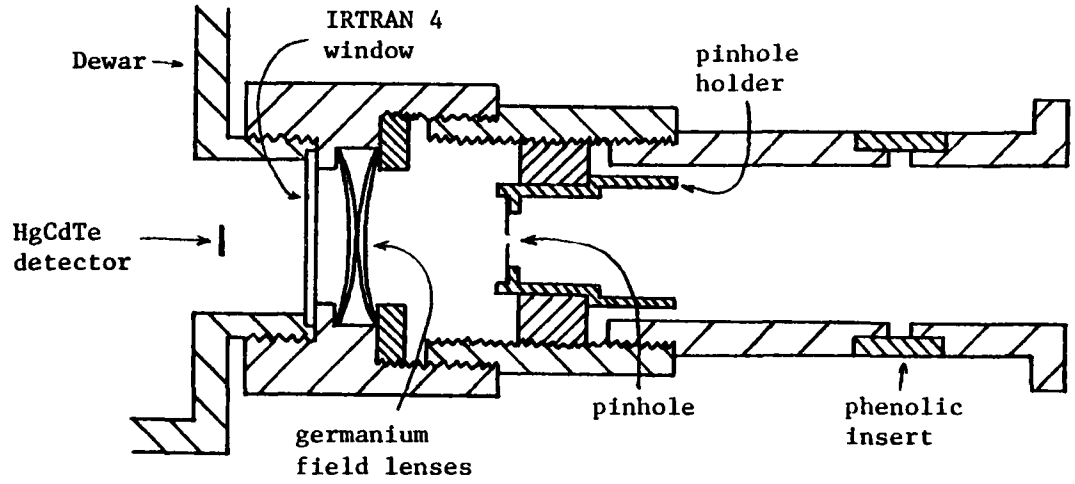


Figure 9. Detector mounting tube

to Figure 10 was used. The dimension W is several times the detector angular subtense to assure good signal response. The heat source was oriented vertically and the target with the horizontal cut was placed in front of it. The temperature of the heat source was adjusted so that it was many times greater than the expected NETD. The signal voltage $V_s$ was determined from an oscilloscope trace of the waveform corresponding to the target. The signal was directed to the oscilloscope from the PAR 113 with the gain and filter settings the same as for the noise voltage measurement. The NETD was then calculated by:

$$NETD = \frac{T_t - T_b}{V_s / V_n}$$

3. MRTD Measurement

The test procedure for determining MRTD involved using the FLIR in its fully operational mode whereby the amplified signal from the detector is applied to the "z" input of the oscilloscope to modulate the electron beam intensity. The heat source and targets were placed 83 meters away and the system was focused for that distance. In the detector mounting tube, the .368 mm pinhole was installed. The initial readings were taken with the lowest frequency four bar target with the bars oriented vertically. The target and background were at the same temperature. At the FLIR video display, the system was adjusted so that noise was clearly visible. The scene brightness was controlled

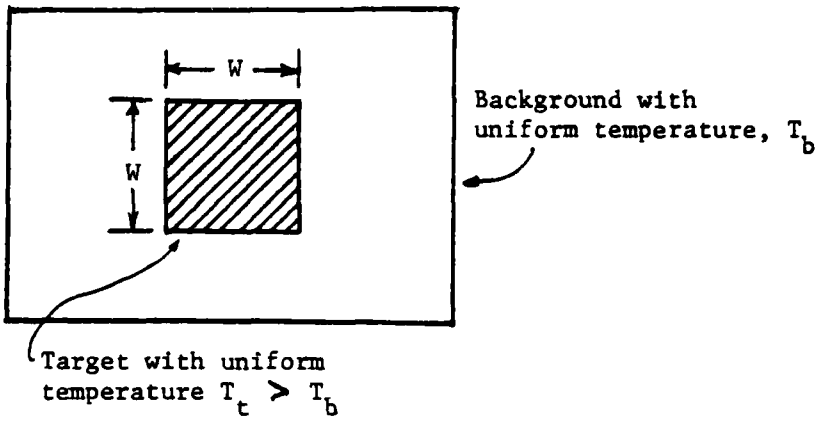


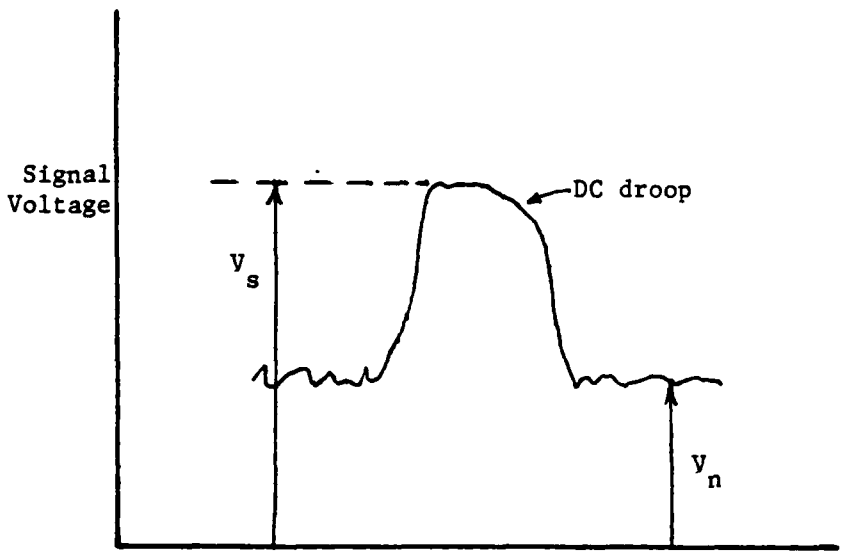


Figure 10. NETD test pattern and resulting voltage waveform

by the intensity adjustment on the oscilloscope and the contrast was controlled by the gain adjustment on the PAR 113 amplifier. The system controls were allowed to be adjusted as the temperature difference between target and background slowly increased until the four bar pattern could confidently be resolved. The establishment of the delta-T is the MRTD evaluated at the spatial frequency of the target. This process was repeated with higher and higher frequencies until the four bar pattern could not be resolved at any temperature. Each pinhole size was tested.

4. MDTD Measurement

The MDTD testing was conducted in two phases. The first phase established the MDTD by subjective means. The procedure involved using the same target as for the NETD test and employed the same technique for target recognition as for the MRTD procedure. The temperature at which target detection occurred established the MDTD at a given spatial frequency as determined by pinhole size. Five sizes of pinholes from .368 mm to 1.5 mm were tested.

The second phase of the MDTD testing involved measuring the signal voltage of the target waveform on an oscilloscope as a function of target temperature. The data from this experiment was plotted to obtain the slope $m = \Delta V_s/\Delta T$. For a unity signal-to-noise ratio, the minimum temperature sensitivity of the system was calculated by $\Delta T = \text{MDTD} = \frac{V_n}{m}$. This process was conducted for all five pinhole sizes.

## IV. PRESENTATION OF DATA

### A. NETD DATA

Table II presents the results of the NETD measurements as a function of pinhole size. A graph of this data is shown in Figure 11. The noise voltage was one millivolt in all cases.

Table II

| Pinhole Size (mm) | NETD (°C) |
|---|---|
| .368 | 14.49 |
| .500 | 7.40 |
| .750 | 5.73 |
| 1.00 | 4.69 |
| 1.50 | 3.08 |

### B. MDTD DATA

Table III presents the results of the first phase of MDTD testing. These points are then plotted as a function of the spatial cutoff frequency of the pinhole size in Figure 12.

Table III

| Pinhole Size (mm) | MDTD (°C) |
|---|---|
| .368 | 76 |
| .500 | 38 |
| .750 | 27 |
| 1.00 | 20 |
| 1.50 | 16 |

The second phase of the MDTD testing was the measuring of the signal voltage as a function of target temperature. These results are given in Figure 13. From these graphs the value of the slope is extracted and used to calculate a delta-T corresponding to the minimum temperature sensitivity (MTS) of the system. Table IV below lists this information.

Table IV

| Pinhole Size (mm) | MTS (°C) |
|---|---|
| .368 | 11.90 |
| .500 | 6.60 |
| .750 | 5.60 |
| 1.00 | 4.43 |
| 1.50 | 2.90 |

C. MRTD DATA

Table V presents the results of the MRTD measurements for each size pinhole. This data is plotted in Figure 14.

Table V

| $f_T(\frac{cy}{mrad})$ | MRTD .368mm | MRTD .50mm | MRTD .75mm | MRTD 1.0mm | MRTD 1.5mm |
|---|---|---|---|---|---|
| 1.73 | 83 | 75 | 31 | 24 | 18 |
| 3.46 | 87 | 80 | 48 | 41 | 35 |
| 6.92 | 191 | 185 | * | * | * |
| 13.83 | * | * | * | * | * |

*Target not resolvable at any temperature

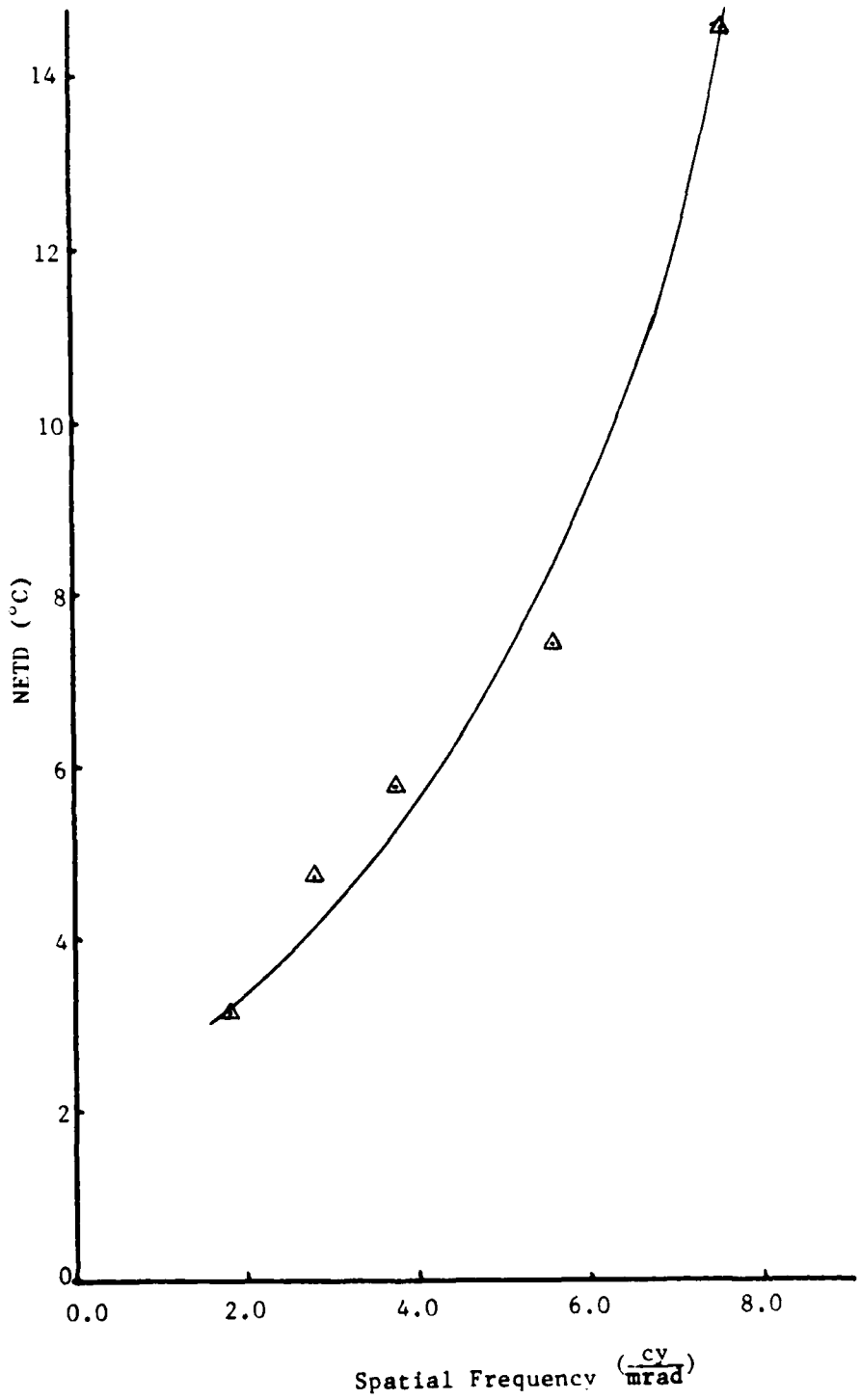


Figure 11. NETD results

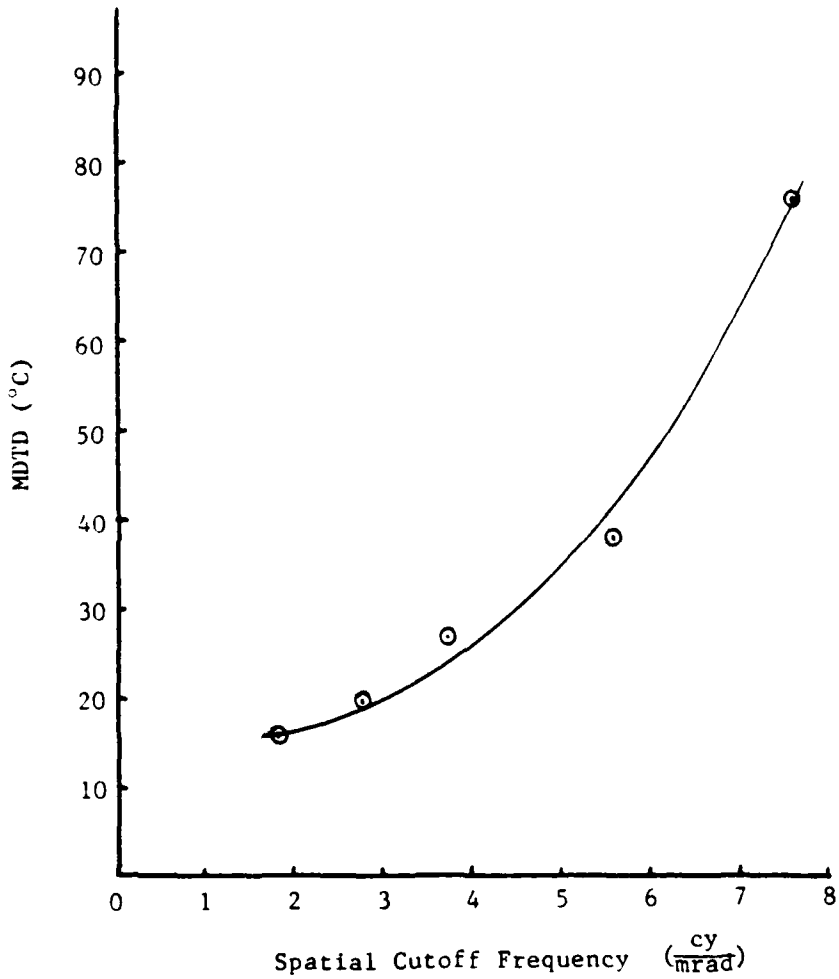


Figure 12. MDTD Results

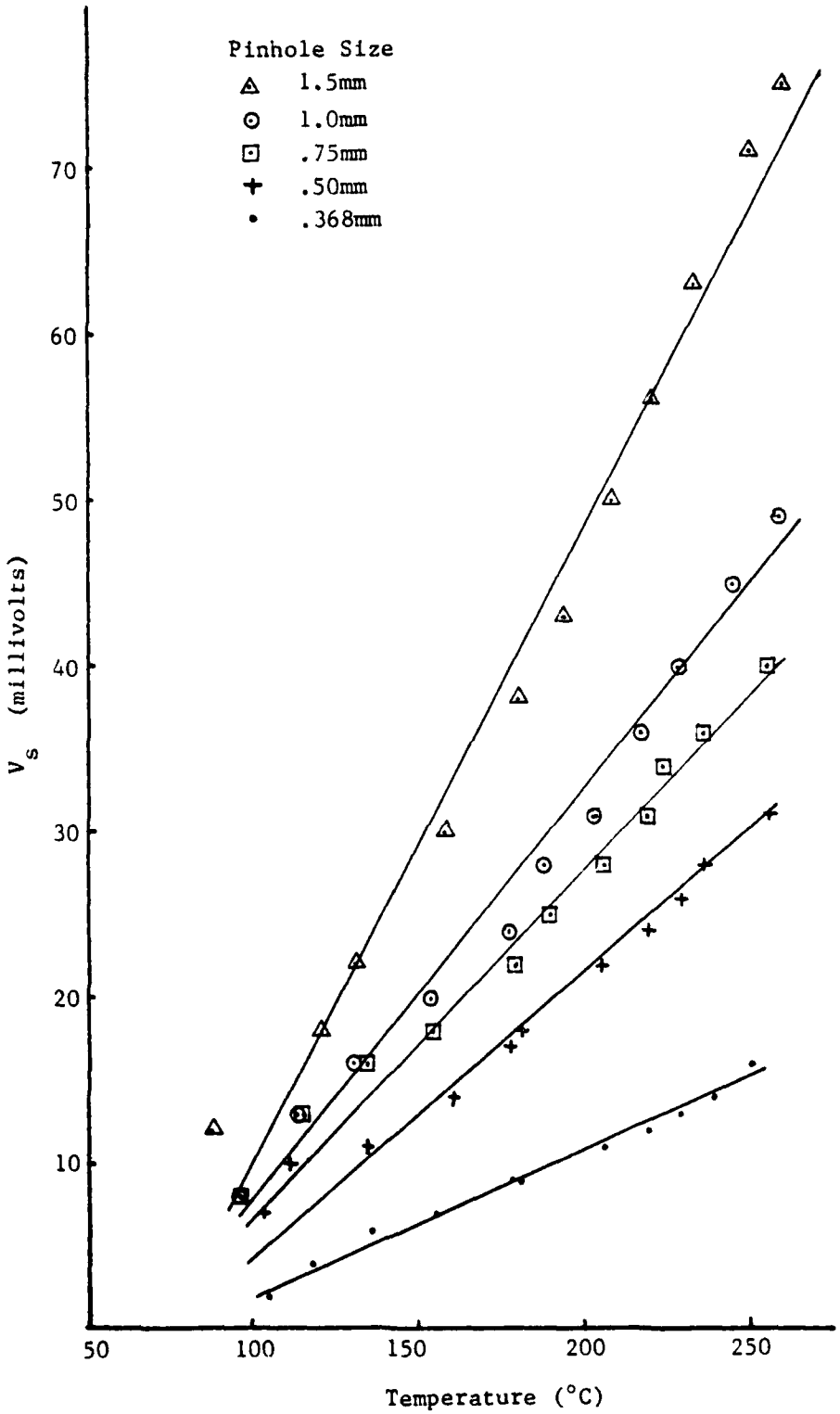


Figure 13. Signal strength versus temperature

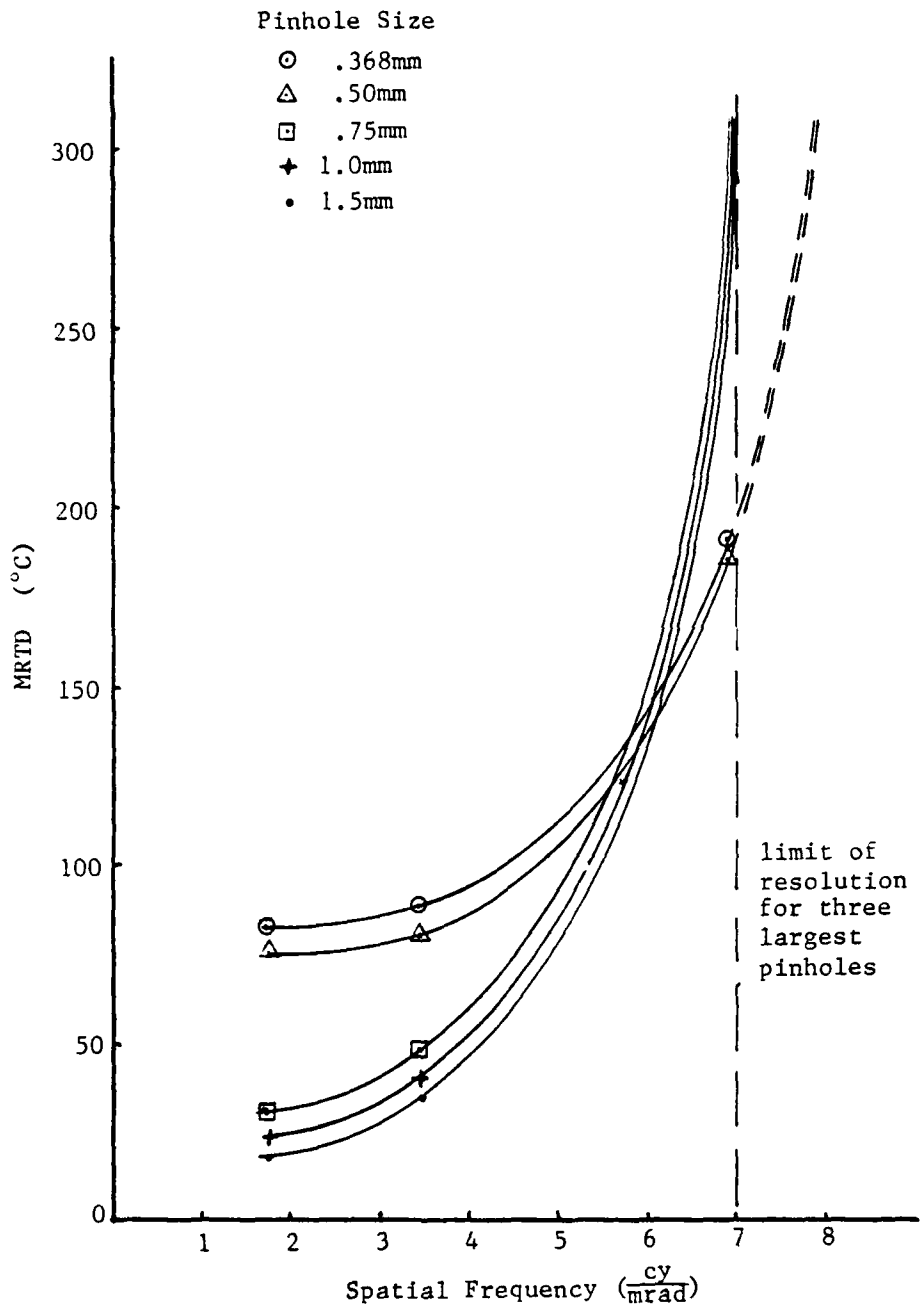


Figure 14. MRTD results

## D. THEORETICAL VALUES

The theoretical value of NETD can be calculated from the previously derived formula for NETD using known or measured values of each parameter. The following is a listing of the constants used for these calculations:

$A_o = 172.8\ cm^2$

$\Delta f_r = 13.5\ KHz$

$\lambda_p = 13\ \mu m$

$T_b = 300\ K$

$\tau_o = .80$

$D^* = 3X10^{10}\ \frac{cm\text{-}Hz^{\frac{1}{2}}}{watt}$

$C_2 = 1.4388X10^4\ \mu m\text{-}K$

$\int_3^{13} W_\lambda(300°)d\lambda = 1.48X10^{-2}\ \frac{watt}{cm^2}$

As the pinhole size changed, the value of $\alpha$, $\beta$, and $A_d$ changed accordingly. Table VI presents the results of the NETD calculations.

Table VI

| Pinhole Size (mm) | NETD (°C) |
|---|---|
| .368 | .61 |
| .500 | .55 |
| .750 | .37 |
| 1.00 | .28 |
| 1.50 | .15 |

The theoretical value for MRTD can be calculated from the previously derived formula for MRTD provided the system MTF has been measured. In the case of the .368mm pinhole, this information is available from an earlier M.S. Thesis. [Gruber, 1979]. Table VII presents these results using the theoretical values of NETD.

Table VII

| $f_T(\frac{cycle}{mrad})$ | MRTD (°C) |
|---|---|
| 1.73 | 2.4 |
| 3.46 | 12.1 |
| 6.92 | 145.3 |
| 13.84 | not resolvable |

# V. CONCLUSIONS

## A. SUMMARY

An analysis of the measured values of the performance parameters reveals several key points concerning the effects of varying the pinhole size. The expected dependence of the thermal sensitivity upon the pinhole size was observed. This was shown by the NETD and MDTD results. The expected increase in optical resolution due to smaller pinhole sizes was observed. This was shown by the MRTD and MDTD results.

The thermal sensitivity demonstrated in the objective tests was not reflected in the values of the thermal sensitivity of the subjective tests. There was considerable loss of thermal sensitivity when the FLIR system was actually used to display thermal images. This was because there are other noise sources and spatial filters in between the point of the subjective measurements and the final image.

The NETD expression can be rearranged to show that NETD is a function of the f-number. Consequently, by varying the pinhole size, the f-number is varied implicitly. This relationship was confirmed by the NETD data.

The theoretical values of NETD and MRTD were not in good agreement with the measured values. It is suspected that the inaccuracy in the theoretical predictions was caused by two factors. First, the emissivity of the target was assumed

to be unity, which it is not. Secondly, the value of the overall transmission coefficient is probably too high. This is perhaps due to the poor reflectance of the telescope mirrors to infrared wavelengths. Since the mirrors are coated with a compound of silicon monoxide, its properties might make it unsuitable for work in the infrared spectrum.

There was good agreement between the NETD results and the minimum temperature sensitivity (MTS) obtained from the slope of the signal strength versus temperature graphs.

## B. COMMENT

The arrangement for the placement of the pinhole was not ideal. A better place to install it would have been directly in front of and next to the detector sensitive area. In this position, it could have been a proper cold shield.

The flyback blanking feature of the FLIR was not connected during system testing. This was not detrimental to target perception or detection.

## BIBLIOGRAPHY


1. Gruber, J. P., Experimental FLIR Study, M.S. Thesis, Naval Postgraduate School, Monterey, California, 1979.

2. Lloyd, J. M., Thermal Imaging Systems, Plenum Press, 1975.

3. Kunz, C. A., Jr., Properties of Detectors for Infrared Transmitting Measurements, M.S. Thesis, Naval Postgraduate School, Monterey, California, 1974.

4. Newbery, A. R. and Worswick, R., "The Laboratory Evaluation of Thermal Imaging Systems", Proceedings of the Society of Photo-Optical Instrumentation Engineers, v. 98, p. 96-104, November 1976.

5. Klein, C. A., "Thermal Imaging Performance of Passive Infrared Scanners", Institute of Electrical and Electronic Engineers Transactions on Geoscience Electronics, v. GE-9, p. 139-146, July 1971.

6. Dereniak, E. L. and Brown, F. G., "NETD Calculations Using the Radiation Slide Rule", Infrared Physics, v. 15, p. 243-248, 1975.

7. Klein, C. A., "NETD Calculations Using the Radiation Slide Rule", Infrared Physics, v. 16, p. 663-664, October 1976.

8. Hudson, R. D., Infrared System Engineering, Wiley, 1969.

9. Barhydt, H., "Effect of F-Number and Other Parameters on FLIR Performance in Nearly BLIP Systems", Optical Engineering, v. 17, p. SR 28-32, March-April 1978.

INITIAL DISTRIBUTION LIST

| | | No. Copies |
|---|---|---|
| 1. | Defense Technical Information Center<br>Cameron Station<br>Alexandria, Virginia 22314 | 2 |
| 2. | Library, Code 0142<br>Naval Postgraduate School<br>Monterey, California 93940 | 2 |
| 3. | Department Chairman, Code 61<br>Department of Physics and Chemistry<br>Naval Postgraduate School<br>Monterey, California 93940 | 2 |
| 4. | Professor E. C. Crittenden, Jr., Code 61Ct<br>Department of Physics and Chemistry<br>Naval Postgraduate School<br>Monterey, California 93940 | 2 |
| 5. | LCDR William L. Sellers, USN<br>USS Greenling (SSN614)<br>FPO, N. Y. 09501 | 1 |

END

DATE
FILMED

8/

DTIC